

Inverse medium problem for a singular contrast

Cite as: J. Math. Phys. **60**, 111508 (2019); <https://doi.org/10.1063/1.5097915>

Submitted: 29 March 2019 . Accepted: 27 October 2019 . Published Online: 25 November 2019

V. Serov, and  T. Tyni

COLLECTIONS

 This paper was selected as an Editor's Pick



View Online



Export Citation



CrossMark

ARTICLES YOU MAY BE INTERESTED IN

[On a center-of-mass system of coordinates for symmetric classical and quantum many-body problems](#)

Journal of Mathematical Physics **60**, 111901 (2019); <https://doi.org/10.1063/1.5119131>

[On the mean field limit for Brownian particles with Coulomb interaction in 3D](#)

Journal of Mathematical Physics **60**, 111501 (2019); <https://doi.org/10.1063/1.5114854>

[Recovery of coefficients in the linear Boltzmann equation](#)

Journal of Mathematical Physics **60**, 111506 (2019); <https://doi.org/10.1063/1.5116899>

Journal of
Mathematical Physics

READ TODAY!

Special Issue: XIXth International
Congress on Mathematical Physics



Inverse medium problem for a singular contrast

Cite as: J. Math. Phys. 60, 111508 (2019); doi: 10.1063/1.5097915

Submitted: 29 March 2019 • Accepted: 27 October 2019 •

Published Online: 25 November 2019



V. Serov^{1,a)} and T. Tyni^{2,b)} 

AFFILIATIONS

¹Research Unit of Mathematical Sciences, University of Oulu, P.O. Box 3000, FI-90014 Oulu, Finland

²Department of Mathematics and Statistics, University of Helsinki, P.O. Box 64, FI-00014 Helsinki, Finland

^{a)}valeri.serov@oulu.fi

^{b)}teemu.tyni@helsinki.fi

ABSTRACT

We consider an inverse medium problem in two- and three-dimensional cases. Namely, we investigate the problem of reconstruction of unknown compactly supported refractive index (contrast) from L^2 with a fixed positive wave number. The proof is based on the new estimates for the Green-Faddeev function in L^∞ space. The main goal of this work is to prove a uniqueness result in the two- and three-dimensional cases and to discuss some possible constructive methods for solving the problem. Finally, we present some numerical examples to demonstrate the results in two dimensions.

Published under license by AIP Publishing. <https://doi.org/10.1063/1.5097915>

I. FORMULATION OF THE PROBLEM

It is well known (see, for example, Ref. 3, Chaps. 8 and 10) that the propagation of time harmonic acoustic waves (with frequency ω) of small amplitude in a slowly varying inhomogeneous medium can be governed by the following steady-state Helmholtz equation:

$$\Delta u(x) + \frac{\omega^2}{c^2(x)} u(x) = 0, \quad x \in \mathbb{R}^n, \quad n = 2, 3, \quad (1)$$

where $u(x)$ denotes the corresponding amplitude in two or three dimensions, Δ is the multidimensional Laplacian, and $c^2(x)$ is the speed of sound. The wave motion is caused by an incident wave u_0 satisfying the unperturbed linearized equation being scattered by the inhomogeneous medium. Assuming the inhomogeneous region is contained inside a bounded domain $\Omega \subset \mathbb{R}^n$, i.e., $c(x) = c_0 = \text{constant}$ for $x \in \mathbb{R}^n \setminus \Omega$, we can see that the scattering problem under consideration is now modeled by

$$-\Delta u(x) - k_0^2 u(x) = k_0^2 m(x) u(x), \quad (2)$$

where $k_0 = \frac{\omega}{c_0}$ is a fixed wave number, $m(x) = \frac{c_0^2}{c^2(x)} - 1 := n^2(x) - 1$ is a perturbation of the refractive index $n(x)$, and

$$u(x) = u_0(x) + u_{\text{sc}}(x), \quad u_0(x) = e^{ik_0(x,\theta)}, \quad \theta \in \mathbb{S}^{n-1},$$

where the scattered field u_{sc} is required to satisfy the Sommerfeld radiation condition at the infinity,

$$\lim_{r \rightarrow \infty} r^{\frac{n-1}{2}} \left(\frac{\partial u_{\text{sc}}(x)}{\partial r} - ik_0 u_{\text{sc}}(x) \right) = 0, \quad r = |x|. \quad (3)$$

We allow for m to be complex-valued in order to include the possibility that the medium is absorbing. The main practical example (it can be considered as the motivation of this research) concerns to refractive index with an imaginary component. As described in Ref. 3, this is often modeled in the literature by adding a term that is proportional to velocity in Euler's equation, which implies that $n^2(x)$ is now of the form

$$n^2(x) = n_1(x) + i \frac{n_2(x)}{k_0} =: 1 + m(x)$$

such that m has compact support in some bounded domain Ω . It is assumed [for uniqueness purposes of the corresponding boundary value problem, see (10)] that $0 < n_1 \leq 1$, $n_2(x) \geq 0$, that is, $-1 < \text{Re}(m) \leq 0$ and $\text{Im}(m) \geq 0$.

The scattering solutions are the unique solutions of the Lippmann-Schwinger equation

$$u(x) = u_0(x) + k_0^2 \int_{\mathbb{R}^n} G_{k_0}^+(|x-y|)m(y)u(y) dy, \tag{4}$$

where $G_{k_0}^+$ is the outgoing fundamental solution of the operator $(-\Delta - k_0^2)$ in \mathbb{R}^n , i.e., the kernel of the integral operator $(-\Delta - k_0^2 - i0)^{-1}$.

Our basic assumption for refractive index m is that it is a complex-valued function, which belongs to $L^2(\Omega)$ (physically, only the imaginary part of m can have some infinite singularities from L^2 , whereas the real part of m can only have jump singularities). In this case, for any fixed $k_0 > 0$, there is a unique solution u of (4) such that

$$\|u_{sc}\|_{L^s(\mathbb{R}^n)} < \infty \tag{5}$$

for some s depending on the dimension n . More precisely, using the parameterization $v = |m|^{\frac{1}{2}}u$, we may rewrite (4) as

$$v(x) = v_0(x) + k_0^2 \int_{\Omega} K(x,y)m(y)v(y) dy, \tag{6}$$

where $v_0 = |m|^{\frac{1}{2}}u_0$ and $K(x,y) = |m(x)|^{\frac{1}{2}}G_{k_0}^+(|x-y|m_{\frac{1}{2}}(y))$ with $m_{\frac{1}{2}} = \text{sign}(m) |m|^{\frac{1}{2}}$. Since the integral operator with kernel $K(x,y)$ is compact in $L^2(\Omega)$ (see, for example, Ref. 24, Chap. 23), we may apply the Riesz theory to prove the existence and uniqueness of the solution u of Eq. (4). These solutions u_{sc} belong to $L^s(\mathbb{R}^n)$ with $s = 4$ if $n = 3$ and with $s = 6$ if $n = 2$ (see Ref. 24, Chap. 23). Even more is true, these solutions u belong to $W_{p,\text{loc}}^2(\mathbb{R}^n)$ with $p = \frac{4}{3}$ if $n = 3$ and with $p = \frac{3}{2}$ if $n = 2$ (see, for example, Ref. 24, Chap. 23).

The property (5) allows us to conclude that the solution $u(x, k_0, \theta)$ for fixed $k_0 > 0$ admits asymptotically as $|x| \rightarrow \infty$ uniformly with respect to θ the representation

$$u(x, k_0, \theta) = e^{ik_0(x,\theta)} + C_n \frac{e^{ik_0|x|}k_0^{\frac{n-3}{2}}}{|x|^{\frac{n-1}{2}}} A(k_0, \theta', \theta) + O\left(\frac{1}{|x|^{\frac{n+1}{2}}}\right),$$

where $\theta' := \frac{x}{|x|} \in \mathbb{S}^{n-1}$, C_n is a known constant depending only on the dimension n , and the function $A(k_0, \theta', \theta)$ is called the scattering amplitude and is defined by

$$A(k_0, \theta', \theta) := k_0^2 \int_{\Omega} e^{-ik_0(\theta',y)} m(y)u(y, k_0, \theta) dy. \tag{7}$$

In this article, we consider an inverse problem of reconstruction of unknown function m from the knowledge of the scattering amplitude $A(k_0, \theta', \theta)$ for all $\theta', \theta \in \mathbb{S}^{n-1}$. We note that these results work also in the more limited (and important) case of backscattering data $\theta' = -\theta$.

The following theorems hold:

Theorem 1. ($n = 3$) Suppose that $m_j(x) \in L^2(\Omega)$ are such that $\text{Re}(m_j) \leq 0$ and $\text{Im}(m_j) \geq 0$ for $j = 1, 2$ and the corresponding scattering amplitudes are equal to each other

$$A_1(k_0, \theta', \theta) = A_2(k_0, \theta', \theta)$$

for fixed $k_0 > 0$ and for all $\theta', \theta \in \mathbb{S}^2$. Then,

$$m_1(x) = m_2(x)$$

almost every in Ω .

Theorem 2. ($n = 2$) Suppose that $m_j \in L^2(\Omega)$ are such that $\text{Re}(m_j) \leq 0$ and $\text{Im}(m_j) \geq 0$ for $j = 1, 2$ and the corresponding scattering amplitudes are equal to each other

$$A_1(k_0, \theta', \theta) = A_2(k_0, \theta', \theta)$$

for fixed $k_0 > 0$ and for all $\theta', \theta \in \mathbb{S}^1$. Then,

$$m_1(x) = m_2(x) \pmod{H_{\text{loc}}^t(\mathbb{R}^2)}$$

for $t < 1$.

Corollary 1. Suppose all conditions of Theorem 2 are satisfied. If the contrasts m_1 and m_2 contain jumps over some smooth curves, then these curves and the height functions of the jumps are the same for both contrasts m_1 and m_2 .

The proof of this corollary follows from the fact that the difference between the functions m_1 and m_2 in the neighborhood of these curves belongs to the space $H_{\text{comp}}^t(\mathbb{R}^2)$ with any $t < 1$. Since no function in $H^s(\mathbb{R}^2)$, $s > \frac{1}{2}$, can have conormal jumps, we have the claim.

The inverse medium problem (with fixed wave number) is very similar to the fixed energy problem for the Schrödinger operator. In dimensions higher than two, it is well known that the scattering amplitude for a fixed positive energy uniquely determines a compactly supported potential (see Refs. 17, 19, 20, and 2). Recently, Bukhgeim¹ proved the uniqueness result in a two-dimensional fixed energy problem for a bounded potential with compact support from W_p^1 , $p > 2$, and then Lakshmanov and Vainberg¹⁴ proved the uniqueness result for a singular potential from L^p , $p > 2$. Our three-dimensional considerations for the Helmholtz operator generalize earlier studies^{3,17–20,27,28} to a more singular refractive index. It should be noted that the reconstruction of singularities in the two-dimensional case for the Schrödinger operator (using the Born approximation) is known much earlier (see Refs. 29–31, 26, and 22); see also Ref. 21. Again, it must be mentioned that the fixed energy problem for Schrödinger operators, theoretically, is equivalent to the inverse medium problem for the Helmholtz operator with a fixed wave number.

One may also be interested in Ref. 9, where inverse scattering problems for the Helmholtz equation are considered with more limited data. Their approach is different from ours and the idea is to use convexification of a Dirichlet-to-Neumann map. The method is tested with experimental measurement data. In Refs. 8 and 10, the uniqueness in the framework of the proposed approximate model is considered and tested with smooth unknown $n(x)$. The numerical approach in this work is similar to that of Refs. 4 and 25, where inverse problems for the Schrödinger operator are considered. Numerically, in the case of the Helmholtz operator, one has to take into account the size of k_0 (this is not needed with the Schrödinger operator).

II. GREEN-FADDEEV FUNCTION

In order to prove Theorems 1 and 2, we need to investigate the mapping properties of the Green-Faddeev function

$$g_z(x) := \frac{1}{(2\pi)^n} \int_{\mathbb{R}^n} \frac{e^{i(x,\xi)}}{\xi^2 + 2(z,\xi)} d\xi,$$

where $z \in \mathbb{C}^n$ is the n -dimensional complex vector with $(z, z) = 0$. Here and in the sequel, the symbol (\cdot, \cdot) denotes the inner product in \mathbb{R}^n . It can be mentioned that $g_z(x)$ is the fundamental solution of the following operator with constant coefficients:

$$(-\Delta - 2i(z, \nabla))g_z(x) = \delta(x).$$

We assume as before that Ω is a bounded domain in \mathbb{R}^n . We extend f by zero outside of Ω . The following results are proved in Ref. 23.

Lemma 1. There exists constant $c > 0$ depending on γ such that for any $f \in L^2(\Omega)$ and for $|z| > 1$,

$$\|g_z * f\|_{L^\infty(\mathbb{R}^n)} \leq \frac{c}{|z|^\gamma} \|f\|_{L^2(\Omega)}, \tag{8}$$

where symbol $g_z * f$ denotes the convolution of g_z and f , $\gamma < 1$ for $n = 2$, and $\gamma < \frac{1}{2}$ for $n = 3$.

The estimates (8) allow us to prove the existence of complex geometric optics (CGO) solutions to the equation

$$-\Delta v - k_0^2 m(x)v = 0. \tag{9}$$

By CGO solutions, we mean the solutions of this equation of the form

$$v(x, z) = e^{i(x,z)}(1 + R(x, z)),$$

where $z \in \mathbb{C}^n$ with $(z, z) = 0$.

Lemma 2. For $m \in L^2(\Omega)$ and $|z|$ large enough, there exists a unique CGO solution of the Schrödinger equation (9) such that

$$\|R\|_{L^\infty(\mathbb{R}^n)} \leq \frac{Ck_0^2}{|z|^\gamma},$$

where γ is as in Lemma 1 and $C > 0$ is a constant independent of k_0 .

III. PROOF OF THEOREM 1

The proof consists of two steps, following classical lines. The first step is to prove that the equality of Dirichlet-to-Neumann maps

$$\Lambda_1 = \Lambda_2$$

for boundary data on $\partial\Omega$ corresponding to two different refractive indices m_1 and m_2 implies the equality $m_1 = m_2$. The second step is to show that the equality of the scattering amplitudes

$$A_1(k_0, \theta', \theta) = A_2(k_0, \theta', \theta)$$

for fixed $k_0 > 0$ implies the equality of the Dirichlet-to-Neumann maps

$$\Lambda_1 = \Lambda_2.$$

For the first step, we consider the Dirichlet boundary value problem for the homogeneous Schrödinger equation

$$\begin{cases} -\Delta u(x) - k_0^2 m(x)u(x) = 0, & x \in \Omega, \\ u(x) = f(x), & x \in \partial\Omega, \end{cases} \quad (10)$$

with function f from the Sobolev space $H^{\frac{1}{2}}(\partial\Omega)$. Using the Lax-Milgram theorem (see, e.g., Refs. 5 and 24) and the assumption $\text{Re}(m) \leq 0$, we can show that there exists a unique solution $u \in H^1(\Omega)$ (in the weak sense) to (10). Thus, we may define the Dirichlet-to-Neumann map Λ as follows:

$$\Lambda f(x) := \frac{\partial u}{\partial \nu}(x), \quad x \in \partial\Omega,$$

where ν is the outward normal vector at the boundary $\partial\Omega$. This map acts here as

$$\Lambda : H^{\frac{1}{2}}(\partial\Omega) \rightarrow H^{-\frac{1}{2}}(\partial\Omega).$$

The following lemma holds:

Lemma 3. If u_1 and u_2 are the solutions of Dirichlet boundary value problem (10) with m_1 and m_2 and with f_1 and f_2 , respectively, then

$$k_0^2 \int_{\Omega} (m_1(x) - m_2(x))u_1 u_2 \, dx = \int_{\partial\Omega} \left(f_1 \frac{\partial u_2}{\partial \nu} - f_2 \frac{\partial u_1}{\partial \nu} \right) d\sigma(x).$$

In particular, if $f_1 = f_2$ and $\Lambda_1 = \Lambda_2$, then

$$\int_{\Omega} (m_1(x) - m_2(x))u_1 u_2 \, dx = 0. \quad (11)$$

This orthogonality condition (11) holds for any two solutions of the Dirichlet boundary value problem (10). However, we need to use it also for CGO solutions. We proceed as follows:

Extend m_1 and m_2 by zero for $x \in \mathbb{R}^3 \setminus \Omega$. Suppose also that $\Lambda_1 = \Lambda_2$. Now, if u_1 and u_2 are two CGO solutions, then it can be proved (see, for example, Ref. 16) that $u_1 = u_2$ in $\mathbb{R}^3 \setminus \Omega$. Thus,

$$u_1(x) = u_2(x), \quad x \in \partial\Omega,$$

and we can use (11) also for CGO solutions. Denoting now by u_1 and u_2 CGO solutions for m_1 and m_2 , respectively, we have

$$u_1(x, z) = e^{i(x,z)}(1 + R_1(x, z)), \quad u_2(x, \bar{z}) = e^{i(x,\bar{z})}(1 + R_2(x, \bar{z}))$$

with

$$iz = l + i(k + p), \quad i\bar{z} = -l + i(k - p),$$

where $l, k, p \in \mathbb{R}^3$ and are mutually orthogonal. Fix arbitrary k and choose $l, p \rightarrow \infty$ such that

$$|l|^2 = |k|^2 + |p|^2.$$

We obtain from the orthogonality condition (11) that

$$\int_{\Omega} (m_1(x) - m_2(x))(1 + R_1(x, z))(1 + R_2(x, z))e^{2i(x,k)} dx = 0.$$

Since

$$\|R_1\|_{L^\infty(\mathbb{R}^3)} \rightarrow 0, \quad \|R_2\|_{L^\infty(\mathbb{R}^3)} \rightarrow 0, \quad l \rightarrow \infty \quad (p \rightarrow \infty),$$

then using Lebesgue's theorem about dominated convergence, we obtain

$$\int_{\Omega} (m_1(x) - m_2(x))e^{2i(x,k)} dx = 0.$$

This equality holds for all $k \in \mathbb{R}^3$. Hence, we conclude that

$$m_1(x) = m_2(x)$$

almost every in Ω . So, the first step is done. Namely, we proved that the equality of the Dirichlet-to-Neumann maps implies the equality of the refractive indices.

Now we are in the position to make the second step. In order to finish the Proof of Theorem 1, we assume that the support of m belongs to the ball $B_R(0) = \{x \in \mathbb{R}^3 : |x| < R\}$. The scattering solutions u_1, u_2 of the Schrödinger equation (2) satisfy the asymptotic representation ($k_0 > 0$ and fixed) as $|x| \rightarrow \infty$,

$$u_j(x, k_0, \theta) = e^{ik_0(x,\theta)} + C_3 \frac{e^{ik_0|x|}}{|x|} A_j(k_0, \theta', \theta) + O\left(\frac{1}{|x|^2}\right), \quad j = 1, 2.$$

Since

$$A_1(k_0, \theta', \theta) = A_2(k_0, \theta', \theta),$$

then for $|x| \rightarrow \infty$,

$$u_1(x, k_0, \theta) - u_2(x, k_0, \theta) = O\left(\frac{1}{|x|^2}\right).$$

At the same time, these solutions satisfy

$$(\Delta + k_0^2)(u_1 - u_2) = k_0^2(m_2(x)u_2(x) - m_1(x)u_1(x)).$$

Due to the assumptions, we have that

$$\text{supp}(m_1 u_1 - m_2 u_2) \subset B_R(0).$$

Applying some modification of Rellich's lemma (see Ref. 28), we obtain that

$$\text{supp}(u_1 - u_2) \subset B_R(0).$$

This fact implies that

$$u_1(x) = u_2(x), \quad x \in \partial B_R(0),$$

and

$$\frac{\partial u_1}{\partial \nu}(x) = \frac{\partial u_2}{\partial \nu}(x), \quad x \in \partial B_R(0).$$

It remains only to remark that the latter equality is equivalent to the equality

$$\Lambda_1 = \Lambda_2$$

for the ball $B_R(0)$. Applying now the result of the first step, we finally obtain that the equality

$$A_1(k_0, \theta', \theta) = A_2(k_0, \theta', \theta)$$

implies

$$m_1(x) = m_2(x)$$

almost every in Ω . This finishes the Proof of Theorem 1.

IV. PROOF OF THEOREM 2

The geometry of the plane does not allow us to choose nonzero vectors $l, k, p \in \mathbb{R}^2$ such that

$$iz = l + i(k + p), \quad i\bar{z} = -l + i(k - p)$$

and are mutually orthogonal. Due to this “property,” it is impossible in the 2D case to prove the result similar to Theorem 1. That is why we proceed as follows: We define the scattering transform by

$$T(\xi) = k_0^2 \int_{\mathbb{R}^2} e^{i(x,\xi)} m(x)(1 + R(x, z)) dx, \quad |\xi| \geq \sqrt{2}C_0, \quad (12)$$

and the $T(\xi) = 0$ for $|\xi| < \sqrt{2}C_0$, where C_0 is defined in Lemma 2. Here, $z = \frac{1}{2}(\xi - iJ\xi)$ and the matrix J is equal to

$$J = \begin{pmatrix} 0 & 1 \\ -1 & 0 \end{pmatrix}.$$

The main idea here is as follows: the scattering amplitude $A(k_0, \theta', \theta)$ with fixed spectral parameter k_0 uniquely determines the Dirichlet-to-Neumann map Λ (see Refs. 27 and 28 and also the Proof of Theorem 1 of this work), and the Dirichlet-to-Neumann map, in turn, uniquely determines the scattering transform T (12) as a function of ξ (see, for example, Ref. 4). This allows us to introduce the Born approximation for this fixed energy problem.

Definition. The inverse scattering Born approximation $q_B(x)$ of the refractive index m is defined by

$$q_B(x) := F^{-1}(T(\xi))(x),$$

where F^{-1} is the inverse Fourier transform and the equality is understood in the sense of tempered distributions.

If we write now q_B with respect to the solution R , then we obtain that

$$\begin{aligned} q_B(x) &= k_0^2 \frac{1}{(2\pi)^2} \int_{\mathbb{R}^2} e^{-i(\xi,x)} \left(\int_{\Omega} e^{i(y,\xi)} m(y)(1 + R(y, z)) dy \right) d\xi \\ &= k_0^2 m(x) + q_1(x) + q_{\text{rest}}(x) \pmod{C^\infty(\mathbb{R}^2)}, \end{aligned} \quad (13)$$

where the first nonlinear term q_1 from the Born series is equal to

$$q_1(x) = k_0^4 \frac{1}{(2\pi)^2} \int_{\mathbb{R}^2} e^{-i(\xi,x)} \left(\int_{\Omega} e^{i(y,\xi)} m(y) \left(\int_{\Omega} g_z(y-s)m(s) ds \right) dy \right) d\xi$$

and q_{rest} is equal to

$$q_{\text{rest}}(x) = k_0^2 \frac{1}{(2\pi)^2} \int_{\mathbb{R}^2} e^{-i(\xi, x)} \left(\int_{\Omega} e^{i(y, \xi)} m(y) \sum_{j=1}^{\infty} R_j(y, z) dy \right) d\xi$$

with the iterations R_j defined as

$$\begin{aligned} R_0(x, z) &= k_0^2 \int_{\Omega} g_z(x - y) m(y) dy, \\ R_j(x, z) &= k_0^2 \int_{\Omega} g_z(x - y) m(y) R_{j-1}(y, z) dy, \quad j = 1, 2, \dots \end{aligned} \tag{14}$$

Lemma 2 gives a rather simple (but a little bit rough) estimation of the smoothness of q_{rest} . Indeed, since for z large enough $|z| \approx |\xi|$, we obtain immediately that [see (12)]

$$\|q_{\text{rest}}\|_{H^t(\mathbb{R}^2)}^2 \leq C \int_{|\xi| > \sqrt{2}C_0} \frac{(1 + |\xi|^2)^t}{|\xi|^{4t}} d\xi < \infty, \quad t < 1.$$

A more detailed analysis shows (see Ref. 26) that this term q_{rest} is actually everywhere a continuous function. Concerning the first nonlinear term q_1 , we also refer to Ref. 26 where it is proved that function $q_1(x)$ belongs to the Sobolev space $W_r^1(\mathbb{R}^2)$ for any $r < 2$. We are ready now to finish the Proof of Theorem 2. Indeed, since for two different refractive indices m_1 and m_2 the representation (13) holds (with the same inverse scattering Born approximation), we obtain that

$$k_0^2(m_1(x) - m_2(x)) = q_{1, m_2} - q_{1, m_1} + q_{\text{rest}, m_2} - q_{\text{rest}, m_1}$$

belongs to $W_r^1(\mathbb{R}^2) + H^t(\mathbb{R}^2) \pmod{C^\infty(\mathbb{R}^2)}$ with $r < 2$ and $t < 1$. Taking into account the imbedding

$$W_r^1(\mathbb{R}^2) \subset H^t(\mathbb{R}^2),$$

we obtain the needed result. Thus, Theorem 2 is completely proved.

Corollary 2 (Backscattering problem with fixed k_0).

Suppose that $m_j \in L^2(\Omega)$ are such that $\text{Re}(m_j) \leq 0$ and $\text{Im}(m_j) \geq 0$ for $j = 1, 2$, and the corresponding scattering amplitudes are equal to each other

$$A_1(k_0, -\theta, \theta) = A_2(k_0, -\theta, \theta)$$

for fixed $k_0 > 0$ and for all $\theta \in \mathbb{S}^{n-1}$, $n = 2, 3$ (this is backscattering data). Then,

$$m_1(x) = m_2(x), \quad n = 3, \quad m_1(x) = m_2(x) \pmod{H_{\text{loc}}^1}, \quad n = 2.$$

It can be verified that the considerations for backscattering data are completely the same as for the Proof of Theorems 1 and 2 of this work.

Remark. As was mentioned (see also Ref. 26, Theorem 1), the term q_{rest} is a continuous function and the first nonlinear term q_1 belongs (in our concrete case) to the Sobolev space $W_r^1(\mathbb{R}^2)$ for any $r < 2$. That is why we may conclude that there is a little bit better result than that formulated in Theorem 2 of this paper. Namely, the difference $m_1(x) - m_2(x)$ belongs to the Sobolev space $W_{r, \text{loc}}^1(\mathbb{R}^2)$ for any $r < 2$.

V. NUMERICS

We follow the numerical approach of Refs. 4 and 25. In this section, our scattering data will be the scattering transform T . The problem of determining T from the scattering amplitude A is interesting and will be the subject of future research.

To begin, we first need to numerically evaluate the scattering transform. To do this, we compute the iterations R_j from (14) by numerically integrating over the support of m . Due to the logarithmic singularity in g_z on the diagonal (and possible singularities in m), this integration is done by adapting the Kress n -point rectangular rule¹² to the 2D-support. The nodes and weights of the integration routine

$$\int_0^1 f(x)dx \approx \sum_{k=1}^{n-1} a_k x_k$$

on the interval $[0, 1]$ are given by

$$x_k = w\left(\frac{2\pi k}{n}\right), \quad a_k = \frac{2\pi}{n} w'\left(\frac{2\pi k}{n}\right)$$

with the weight function

$$w_p(t) = \frac{t^p}{t^p + (2\pi - t)^p}, \quad p = 3,$$

see, e.g., Refs. 11 and 12. Here, the integral may have singularities only at the end-points. If the singularity occurs at some $a \in]0, 1[$, we adapt by considering instead the intervals $[0, a]$ and $[a, 1]$. In our examples, we used two iterations,

$$R \approx R_0 + R_1.$$

Since the functions R_j are bounded, the calculation of T is easier: we need to only worry about possible singularities of m . It should be mentioned that the evaluation of the Faddeev's Green function g_z is done by using the exponential integral method (for details see, for example, Sec. 14.3.2 of Ref. 15).

Having obtained the synthetic measurement data T , we can start the inversion. Our approach is to consider the inverse Born approximation q_B as the unknown, in the sense that we do not directly calculate the Fourier transform of the data $T(\xi)$, but rather solve a linear system that gives q_B as its solution. More precisely, since

$$q_B(x) := F^{-1}(T(\xi))(x),$$

then by Fourier inversion,

$$T(\xi) = F(q_B)(\xi) = \int_{\mathbb{R}^2} e^{i(x,\xi)} q_B(x) dx.$$

We will now form a piecewise constant approximation of q_B , where the values of q_B inside the pixels are unknown. We divide our reconstruction grid into N pixels and denote each pixel by r_j . Then, we substitute instead of q_B the piecewise constant form

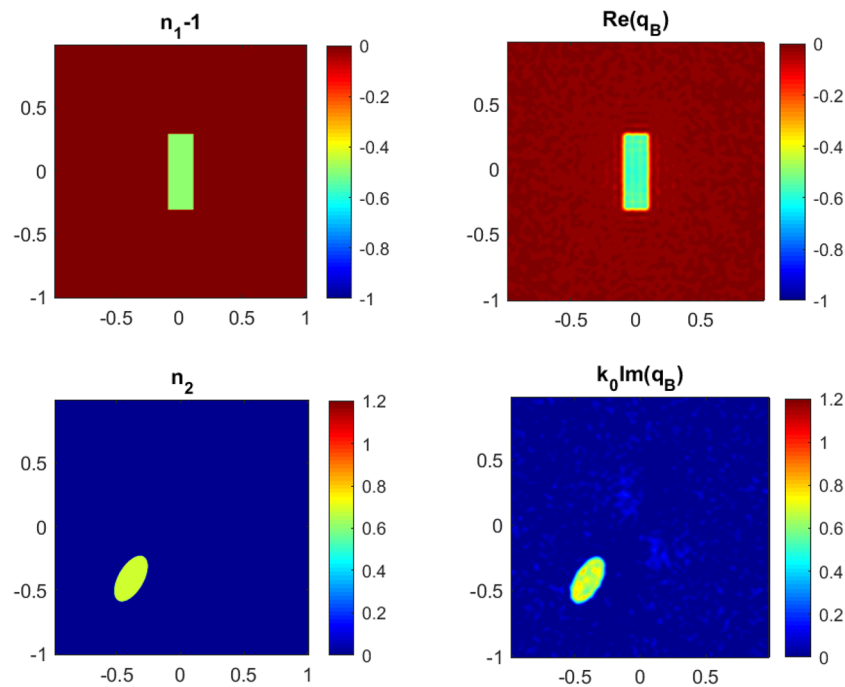


FIG. 1. Example 1: Precise unknown left and the CGLS reconstruction right with the real part above and the imaginary part below.

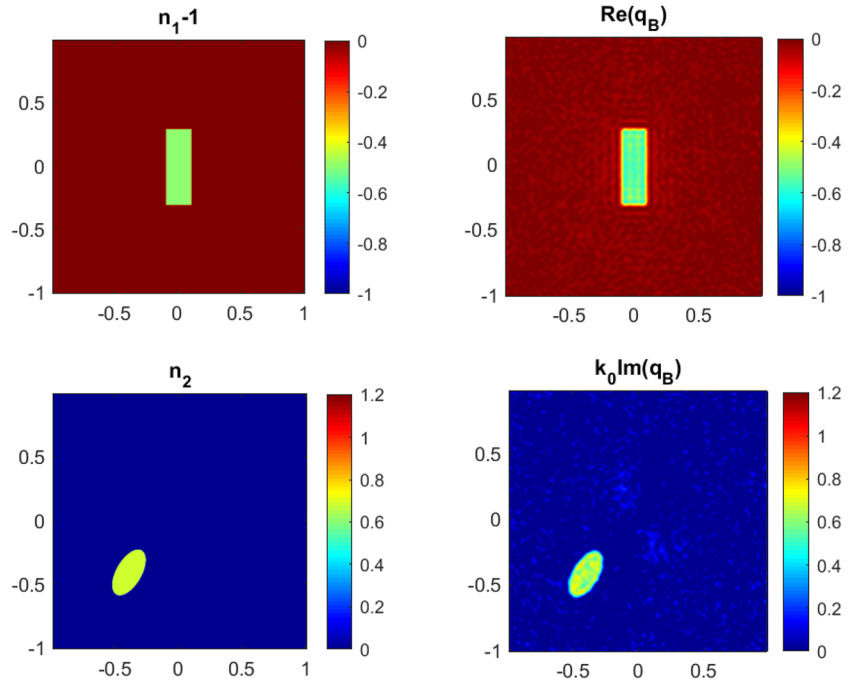


FIG. 2. Example 1: Precise unknown left and the Tikhonov reconstruction right with the real part above and the imaginary part below.

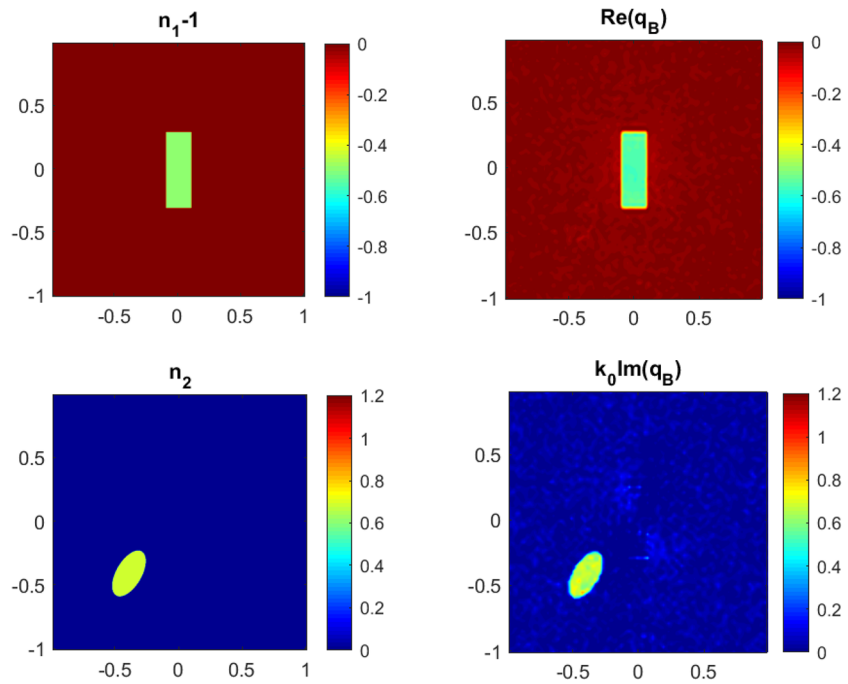


FIG. 3. Example 1: Precise unknown left and the TV reconstruction right with the real part above and the imaginary part below.

$$q_B(x) \approx \sum_{j=0}^N f_j \chi_{r_j}(x),$$

where χ_{r_j} are the characteristic functions of the pixels and f_j are the unknown values of q_B in r_j . Doing this, we obtain

$$T(\xi) = \sum_{j=0}^N f_j \int_{r_j} e^{i(x,\xi)} dx + \delta(\xi),$$

where we ignore the error term $\delta(\xi)$. The above integrals can be easily computed in closed form by hand. Now conducting measurements at M points ξ_k , we arrive to the linear problem $Ef = g$, where $g_k = T(\xi_k)$ are the measurements and the matrix $E \in \mathbb{C}^{M \times N}$ contains the values of the above integrals. One can think of this linear system as a linear inverse problem and use some inverse problems methods to solve it. In fact, we always choose the number of unknowns $M < N$ so that this linear system is under-determined, ill-conditioned, and rank-deficient, which means that regularization methods are necessary.

This approach of regarding q_B as the unknown has the benefit of easily allowing one to choose the regularization method. Note also that there is no danger of committing inverse crime, since the measurement data T is obtained from the CGO-solutions by numerically integrating R . The inversion on the other hand is done in a completely separate reconstruction grid.

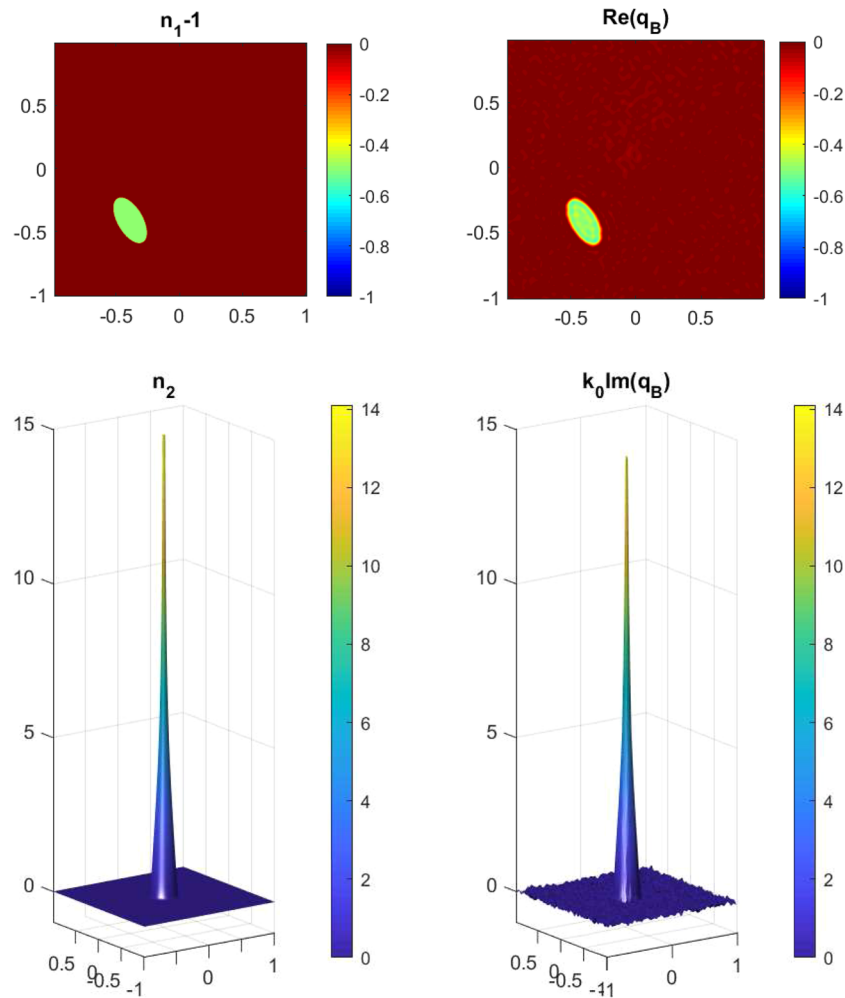


FIG. 4. Example 2: Precise unknown left and the CGLS reconstruction right with the real part above and the imaginary part below.

A. Regularization

We tested three (actually four) different regularization methods: the conjugate gradient least squares (CGLS), Tikhonov, and total variation (TV) regularization methods. Between these three, the CGLS- and TV-methods seem to work best for recovering jumps and singularities in the presence of infinite singularities. Tikhonov regularization works well, when the components of the refractive index are small (in L^2 -norm). We also tested the truncated singular value decomposition approach to regularize the problem, but in our experiments, this method did not work so well.

The CGLS-method is an iterative approach to minimizing the expression

$$\arg \min \{ \|E f_k - g\|_2 \}$$

under the constraint $f_k \in \{E^* g, \dots, (E^* E)^{k-1} E^* g\}$. This method focuses on the significant singular components. We used the CGLS-algorithm of Hestenes and Stiefel (see, e.g., Refs. 6 and 7).

The Tikhonov regularization instead aims to minimize the expression

$$\arg \min \{ \|E f - g\|_2^2 + \lambda \|f\|_2^2 \},$$

where $\lambda > 0$ is the regularization parameter (see, e.g., Refs. 6 and 15). This method works rather well for our problem when the L^2 -norm of our solution is relatively small. However, in our case, in the presence of infinite singularities, this method picks too small solutions.

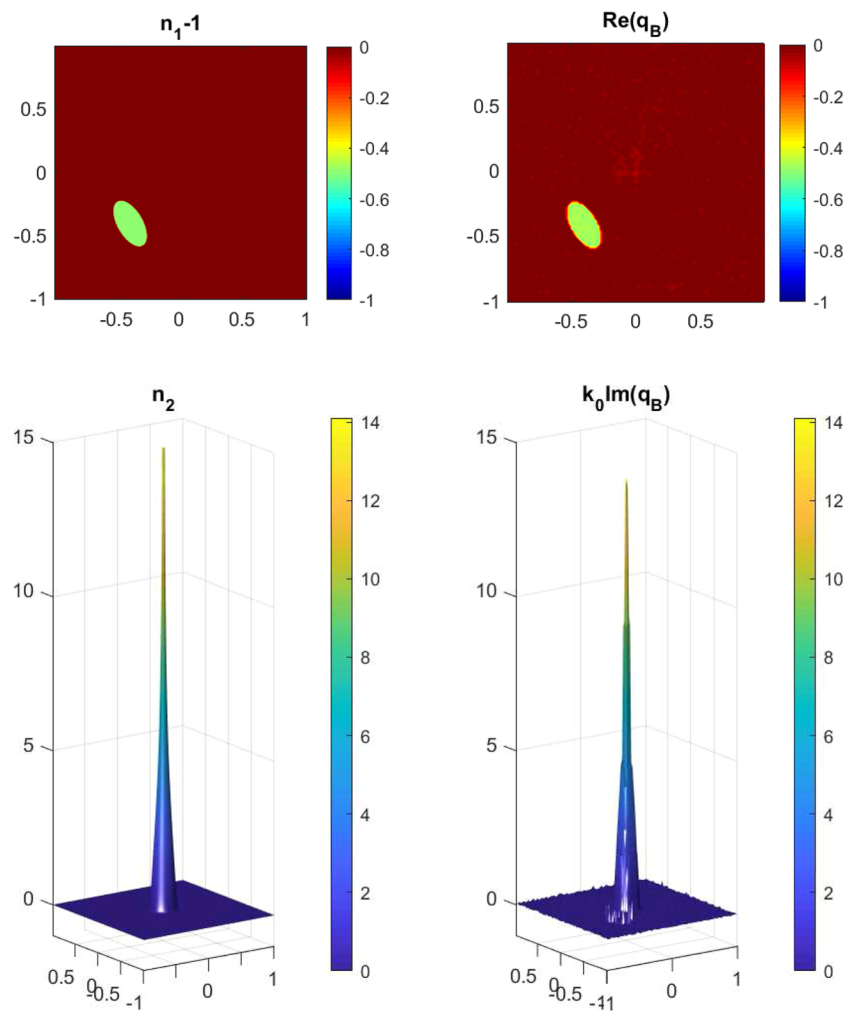


FIG. 5. Example 2: Precise unknown left and the TV reconstruction right with the real part above and the imaginary part below.

Finally, in TV-regularization, we use a little different penalty term and minimize the expression

$$\arg \min \{ \|Ef - g\|_2^2 + \lambda \|\nabla f\|_1 \}.$$

This method allows the solution f to have some steep gradients and hence works rather well when reconstructing jumps and infinite singularities. The downside is that this method is somewhat complicated to implement. We use the approach described in Ref. 15 with some modifications to allow for complex matrix E and solution f . In addition, since we *a priori* assume that the solution f satisfies $-1 < \operatorname{Re}(f) \leq 0$ and $\operatorname{Im}(f) \geq 0$, we can use these conditions as constraints to help find the optimized solution.

B. Numerical examples

In all of the following examples, $m(x) = n_1(x) - 1 + \frac{i}{k_0} n_2(x)$ and $k_0 = 5$. As shown in Lemma 2, the size of R depends on k_0 . Therefore, to obtain visually good reconstruction, we need to use large enough measurement points (in modulus) to compensate for the size of k_0 . We used $M = 8100$ measurement points in a $[-100, 100]^2$ square grid. If k_0 is smaller (say, $k_0 = 1$), then a smaller grid suffices. The number of unknown values f_j is $N = 10^4$ and we attempt to recover m in a $[-1, 1]^2$ square. In all of the examples, the measurement data are corrupted by Gaussian white noise with standard deviation of 1% of the maximum of the measurements.

The generation of the synthetic measurements T for one example with two iterations takes about 15 hours on a computer with 20 core CPU at 2.2 GHz. In the future, we are interested in trying finite element methods for the direct problem so that one does not need to iterate

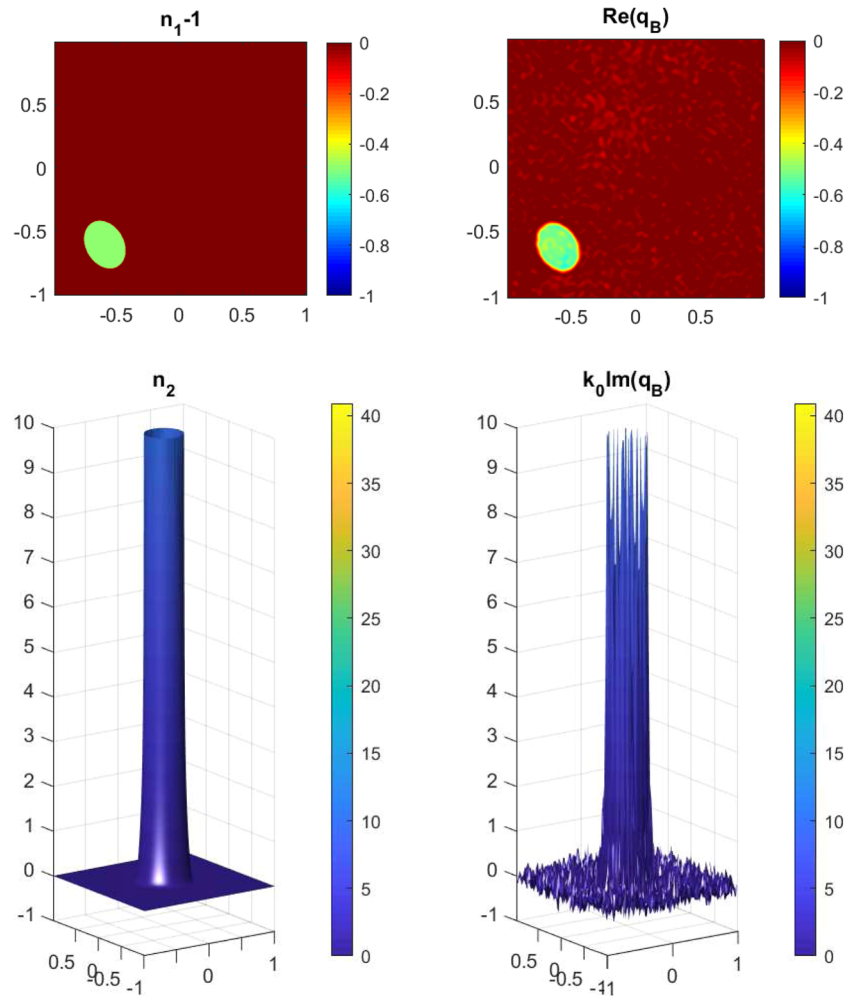


FIG. 6. Example 3: Precise unknown left and the CGLS reconstruction right with the real part above and the imaginary part below.

the numerically expensive integral equation. The inversion methods are much quicker. The CGLS solutions can be computed in less than a second, while Tikhonov solutions take few minutes. The TV method is the slowest. The numerical work is done in MATLAB.

Example 1. Let $m(x) = -0.5\chi_{\text{rectangle}}(x) + \frac{0.7}{k_0}\chi_{\text{ellipse}}(x)$.

Example 2. Let

$$m(x) = -0.5\chi_{\text{ellipse}}(x) - \frac{i\phi_{|x|<0.3}(x)}{k_0|x|\log(|x|)}.$$

Example 3. Let

$$m(x) = -0.5\chi_{\text{ellipse}}(x) + \frac{i\phi_{|x|<0.3}(x)}{k_0|0.25-|x||^{0.4}}.$$

Here, $\chi(x)$ is the characteristic function and $\phi_{|x|<0.3}$ is a smooth bump function supported in the ball $|x| < 0.3$.

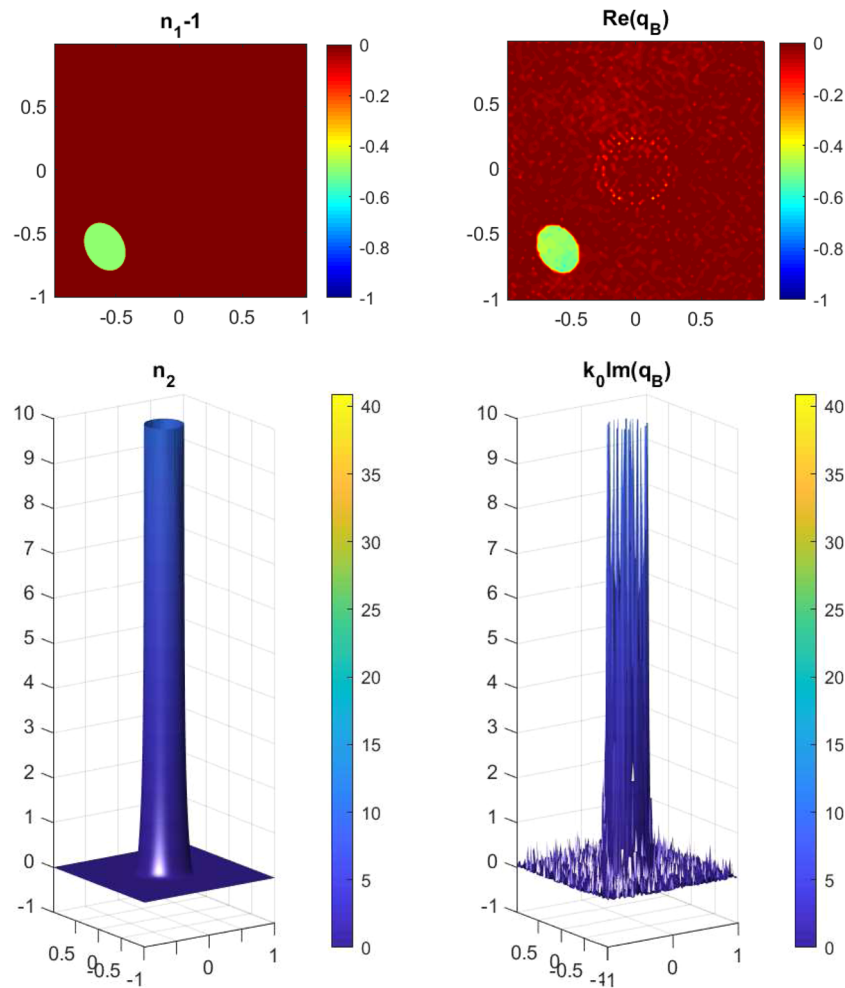


FIG. 7. Example 3: Precise unknown left and the TV reconstruction right with the real part above and the imaginary part below.

Figures 1–3 demonstrate the recovery of shapes (with possible corners), while in Figs. 4–7, we attempt to detect infinite singularities. The singularity in Example 2 is rather small and supported at a single point, while the large singularity of Example 3 is spread on the circle with radius 0.25. Note that in Figs. 4–7, we plot only a small portion of the infinite singularity.

VI. CONCLUSIONS AND DISCUSSION

Remark. One could also try to introduce the inverse Born approximation for this problem. It could be defined (using a similar procedure as for the Schrödinger operator with not fixed wave number k^2) by (consider for simplicity only $n = 3$)

$$\begin{aligned} q_B(x) &:= \int_{\mathbb{S}^2} \int_{\mathbb{S}^2} e^{-ik_0(x, \theta - \theta')} A(k_0, \theta', \theta) d\theta d\theta' \\ &= k_0^2 \int_{\Omega} m(y) dy \int_{\mathbb{S}^2} \int_{\mathbb{S}^2} e^{-ik_0(x, \theta - \theta')} e^{-ik_0(y, \theta')} u(y, k_0, \theta) d\theta d\theta' \\ &= k_0^2 \int_{\Omega} m(y) dy \int_{\mathbb{S}^2} \int_{\mathbb{S}^2} e^{-ik_0(x-y, \theta - \theta')} d\theta d\theta' + k_0^4 e^{ik_0|x|} O\left(\frac{1}{|x|}\right), \quad |x| > 1, \end{aligned}$$

where O is uniform with respect to θ and θ' . The first term in the latter sum can be calculated (using the knowledge of Bessel functions) precisely (see Ref. 13) and it is equal to

$$q_B(x) \approx 16\pi^2 \int_{\Omega} \frac{m(y) \sin^2(k_0|x-y|)}{|x-y|^2} dy.$$

It is clear that this term is a bounded continuous function in $x \in \mathbb{R}^3$ and behaves as $O^*\left(\frac{1}{|x|^2}\right)$ at the infinity. These facts show that the inverse scattering Born approximation does not contain any significant information about the contrast m (for example, singularities of m) and, therefore, cannot be used in the reconstruction of singularities (jumps) of unknowns.

We considered an inverse medium problem with possibly singular contrast (refractive index) in dimensions two and three. The main motivation was to account for possibly absorbing medium, where the refractive index is allowed to be complex-valued. The real part of the refractive index is bounded, but the imaginary part can have infinite singularities from L^2 . The main theorems are uniqueness theorems for the inverse scattering problem with a fixed wave number: equality of the scattering amplitudes (the measurement data) implies the equality of the corresponding refractive indices. These results also hold under the backscattering data, where measurements are made in the opposing direction of the incident field. We also demonstrate the results numerically. We presented several examples, where we attempt to recover the location of a compactly supported refractive index with a nonzero imaginary part. In the numerical approach, we have to take into account the size of the wave number k_0 , in contrast with the corresponding numerical results for the Schrödinger operator. Examples where the imaginary part of the refractive index has singularities at a point and along a surface are also given.

ACKNOWLEDGMENTS

This work was supported by the Academy of Finland (Application No. 312123, Finnish Programme for Centres of Excellence in Inverse Modelling and Imaging 2018–2025).

REFERENCES

- A. L. Bukhgeim, “Recovering a potential from Cauchy data in the two-dimensional case,” *J. Inverse Ill-Posed Probl.* **16**, 19–33 (2008).
- S. Chanillo, “A problem in electrical prospection and n -dimensional Borg-Levinson theorem,” *Proc. Am. Math. Soc.* **108**, 761–767 (1990).
- D. Colton and R. Kress, *Inverse Acoustic and Electromagnetic Scattering Theory*, 3rd ed. (Springer, New York, 2013).
- G. Fotopoulos and V. Serov, “Inverse fixed energy scattering problem for the two-dimensional nonlinear Schrödinger operator,” *Inverse Probl. Sci. Eng.* **24**(4), 692–710 (2016).
- D. Gilbarg and N. S. Trudinger, *Elliptic Partial Differential Equations of Second Order*, 2nd ed. (Springer, Berlin, 1983).
- P. C. Hansen, *Discrete Inverse Problems: Insight and Algorithms* (SIAM, USA, 2010).
- M. R. Hestenes and E. Stiefel, “Methods of conjugate gradients for solving linear systems,” *J. Res. Natl. Bur. Stand.* **49**, 409–436 (1952).
- M. V. Klivanov, “Convexification of restricted Dirichlet-to-Neumann map,” *J. Inverse Ill-Posed Probl.* **25**, 669–685 (2017).
- M. V. Klivanov, A. E. Kolesov, and D.-L. Nguyen, “Convexification method for an inverse scattering problem and its performance for experimental backscatter data for buried targets,” *SIAM J. Imaging Sci.* **12**, 576–603 (2019).
- M. V. Klivanov, J. Li, and W. Zhang, “Convexification of electrical impedance tomography with restricted Dirichlet-to-Neumann map data,” *Inverse Probl.* **35**, 035005 (2019).

- ¹¹R. Kress, “Nyström method for boundary integral equations in domains with corners,” *Numer. Math.* **58**, 145–161 (1990).
- ¹²R. Kress, *Numerical Analysis* (Springer, New York, 1998).
- ¹³N. N. Lebedev, *Special Functions and Their Applications* (Dover Publications, New York, 1972).
- ¹⁴E. Lakshtanov and B. Vainberg, “Recovery of L^p -potential in the plane,” *Inverse Ill-Posed Probl.* **25**, 633–651 (2017).
- ¹⁵J. L. Mueller and S. Siltanen, *Linear and Nonlinear Inverse Problems with Practical Applications* (SIAM, USA, 2012).
- ¹⁶A. Nachman, J. Sylvester, and G. Uhlmann, “An n -dimensional Borg-Levinson theorem,” *Commun. Math. Phys.* **115**, 595–605 (1988).
- ¹⁷A. I. Nachman, “Reconstruction from boundary measurements,” *Ann. Math.* **128**, 531–576 (1988).
- ¹⁸A. I. Nachman, “Global uniqueness for a two dimensional boundary value problem,” *Ann. Math.* **143**, 71–96 (1996).
- ¹⁹A. I. Nachman, “Inverse scattering at fixed energy,” in *Proceedings 10th International Conference on Applied Physics and Mathematics (Leipzig, August 1991)* (Springer, Berlin, 1992).
- ²⁰R. G. Novikov, “Multidimensional inverse spectral problem for the equation $-\Delta\psi + (v(x) + Eu(x))\psi = 0$,” *Funct. Anal. Appl.* **22**, 263–272 (1988).
- ²¹R. G. Novikov, “The inverse scattering problem on a fixed energy level for the two-dimensional Schrödinger operator,” *J. Funct. Anal.* **103**, 409–463 (1992).
- ²²L. Päiväranta and V. Serov, “An n -dimensional Borg-Levinson theorem for singular potentials,” *Adv. Appl. Math.* **29**, 509–520 (2002).
- ²³V. Serov, “Inverse fixed energy scattering problem for the generalised nonlinear Schrödinger operator,” *Inverse Probl.* **28**, 025002 (2012).
- ²⁴V. Serov, *Fourier Series, Fourier Transform and Their Applications to Mathematical Physics* (Springer, New York, 2017).
- ²⁵V. Serov, M. Harju, and G. Fotopoulos, “Some recent advances in nonlinear inverse scattering in 2D: Theory and numerics,” in *Appeared in Applied Linear Algebra in Action* (Intech, Croatia, 2016), pp. 115–137.
- ²⁶V. Serov and L. Päiväranta, “New estimates of the Green-Faddeev function and recovering of singularities in the two-dimensional Schrödinger operator with fixed energy,” *Inverse Probl.* **21**, 1291–1301 (2005).
- ²⁷J. Sylvester, “The Cauchy data and the scattering amplitude,” *Commun. PDE* **191**, 735–741 (1994).
- ²⁸J. Sylvester, “Inverse boundary value problems: An overview,” *Algebra I Anal.* **8**, 195–204 (1996).
- ²⁹Z. Sun and G. Uhlmann, “Inverse scattering for singular potentials in two dimensions,” *Trans. Am. Math. Soc.* **338**, 363–374 (1993).
- ³⁰Z. Sun and G. Uhlmann, “Recovery of singularities for formally determined inverse problems,” *Commun. Math. Phys.* **153**, 431–445 (1993).
- ³¹T. Y. Tsai, “The Schrödinger operator in the plane,” *Inverse Probl.* **9**, 763–787 (1993).